RESEARCH PAPER

CuO/ZnO@N-GQDs@NH_2 nanocomposite as superior catalyst for the synthesis of pyrimidine-triones

Hossein Shahbazi-Alavi[1,*], Seyyed Mohammad Ebrahimi[2], Javad Safaei-Ghomi [3]

[1] Young Researchers and Elite Club, Kashan Branch, Islamic Azad University, Kashan, Iran.

[2] Department of Organic Chemistry, Faculty of Chemistry, University of Kashan, Kashan, Iran

ARTICLE INFO

Article History:
Received 04 January 2021
Accepted 26 February 2021
Published 15 March 2021

Keywords:
Nanocatalyst
Pyrimidines
One-pot
Nanocomposite
CuO/ZnO

ABSTRACT

CuO/ZnO@N-GQDs@NH_2 nanocomposite (copper(II) oxide/zinc oxide@ nitrogen-doped graphene quantum dots @aminated) as superior catalyst was applied for the synthesis of pyrimidine-trions by three-component reactions of N,N-dimethylbarbituric acid, benzaldehydes and para-methyl aniline or para-methoxy aniline under reflux condition in water. The catalyst was characterized by SEM (scanning electron microscope), FT-IR (Fourier-transform infrared spectroscopy), XRD (X-ray powder diffraction), TGA (thermogravimetric analysis), EDS (Energy-dispersive X-ray spectroscopy), and XPS (X-ray photoelectron spectroscopy). The best results were gained in H2O and we found the convincing results for the synthesis of pyrimidine-trions in the presence of CuO/ZnO@N-GQDs@NH_2 nanocomposite (5 mg) under reflux conditions. This technique provides several benefits including green reaction conditions, great yields in concise times, a retrievable nanocatalyst, and low nanocatalyst loading.

How to cite this article
Shahbazi-Alavi H.; Ebrahimi SM.; Safaei-Ghomi J. CuO/ZnO@N-GQDs@NH_2 nanocomposite as superior catalyst for the synthesis of pyrimidine-triones. Nanochem Res, 2021; 6(1):10-17. DOI: 10.22036/ncr.2021.01.002

INTRODUCTION

Pyrimidines show anti-cancer [1], glucosidase inhibitor [2], antioxidant [3], anti-microbial [4] and anaesthetic activities [5]. The detection of an effective procedure for the synthesis of pyrimidines is a drastic challenge. The preparation of pyrimidines has been studied using catalysts including Indium(III) chloride [6], tungstophosphoric acid [7], potassium carbonate [8], tosylic acid [9] and 1-N-butyl-3-methylimidazolium hexafluorophosphate [10]. Each of these procedures may have its own advantages, but also suffer from apparent drawbacks such as prolonged reaction times, complicated work-up, low yield, or hazardous reaction conditions. Despite the availability of these ways, there remains enough choice for a capable and reusable catalyst with high catalytic activity for the preparation of pyrimidines. Metal oxides represent a wide class of materials that have been researched significantly due to their unique attributes, and they are used in many fields [11-12]. Graphene quantum dots (GQDs) have gained intensive attention owing to the remarkable features [13-14]. Potential applications of GQDs were recently reviewed on the basis of experimental and theoretical investigations [15-16]. Preparation of highly efficient nanocomposite catalysts for the synthesis of organic compounds is still an attractive challenge. To attain larger surface area, nanocatalysts are functionalized by active groups [17-18]. The decoration of the nanoparticles with GQDs prevents the aggregation of fine particles and thus increases the efficient surface area and number of reactive sites for an effective catalytic reaction [19-20]. Recently the use of environmental and green catalysts which can be easily recycled has received significant attention. Besides, environmental advantages, such recoverable catalysts can also provide a platform for heterogeneous catalysis, green chemistry, and

* Corresponding Author Email: *hosseinshahbazi99@yahoo.com*

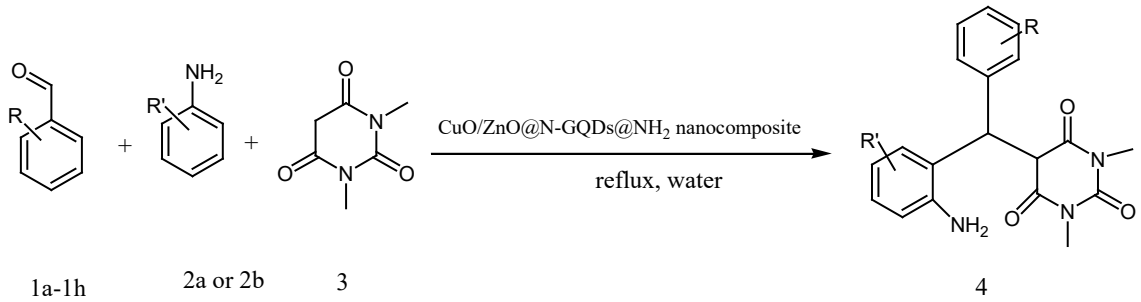

Scheme 1. Synthesis of pyrimidine-triones

environmentally benign protocols in the near future [21-23]. Herein, we report the use of CuO/ZnO@N-GQDs@NH_2 nanocomposite as effective catalyst for the preparation of pyrimidine-trions by three-component reactions of N,N-dimethylbarbituric acid, benzaldehydes and 4-methyl aniline or 4-methoxy aniline under reflux condition in water (Scheme 1).

EXPERIMENTAL

Chemicals and apparatus

All organic materials were purchased commercially from Sigma-Aldrich and Merck. Powder X-ray diffraction (XRD) was performed on a Philips diffractometer of X'pert Company with monochromatized Cu Kα radiation (λ = 1.5406 Å). Microscopic morphology of nanocatalyst was visualized by SEM (MIRA3). The thermogravimetric analysis (TGA) curves are registered by V5.1A DUPONT 2000. The IR spectra were recorded on FT-IR Magna 550 apparatus using with KBr plates. The Energy-Dispersive X-ray Spectroscopy (EDS) measurement was carried out with the SAMX analyzer. X-ray photoelectron spectroscopy (XPS) spectra were measured on an ESCA-3000 electron spectrometer. NMR spectra were obtained by a Bruker 400 MHz spectrometer (^{1}H NMR at 400 Hz, ^{13}C NMR at 100 Hz) in DMSO-d_6 using TMS as an internal standard.

Preparation of CuO/ZnO nanoparticles

$Cu(OAC)_2{\cdot}2H_2O$ and $Zn(OAC)_2{\cdot}4H_2O$ in a 1:1 molar ratio were dissolved in deionized water. Afterward, the appropriate amount of aqueous sodium hydroxide solution (0.70 M) was added to the above solution until the pH value reached 10. Then, the transparent solution was placed in an autoclave at 120 °C for 5 h. The obtained precipitate was washed twice with methanol and dried at 70 °C for 4 h. Finally, the product was calcined at 600 °C for 3 h.

Preparation of CuO/ZnO@N-GQDs nanocomposite

Citric acid (1.0 g) was dissolved in 20 mL deionized water, and stirred to form a clear solution. After that, 0.3 mL ethylene diamine was added. Then, 0.10 g CuO/ZnO nanoparticles were added to the mixture. The mixture was stirred at room temperature for 5 minutes. Then, the solution was transferred to a 50 mL Teflon lined stainless steel autoclave. The sealed autoclave was heated to 180°C for 9 hours in an electric oven. Finally, the nanostructured CuO/ZnO @ N-GQDs were obtained, washed several times with deionized water (10 mL) and ethanol (10 mL), and then dried in an oven at 70 °C until constant weight was achieved.

Preparation of CuO/ZnO@N-GQDs@NH_2 nanocomposite

The CuO/ZnO@N-GQDs nanocomposite (1.0 g) was added to a solution of 3-aminopropyltriethoxysilane (2.0 mmol, 0.44 g) in dry toluene (20 mL) and refluxed for 24 h. After the reaction was complete, the aminated-CuO/ZnO@N-GQDs were separated using a centrifuge, washed with double-distilled water (10 mL) and anhydrous ethanol (10 mL), and dried at 80 °C for 8 h to give the nanocomposite having surface bound amino groups, CuO/ZnO@N-GQDs@NH_2.

General procedure for the synthesis of pyrimidines

A mixture of N,N-dimethylbarbituric acid (1 mmol), benzaldehydes (1 mmol) and para-methyl aniline or para-methoxy aniline (1 mmol) and CuO/ZnO @N-GQDs@NH_2 nanocomposite (5 mg) was heated in water (5 mL) under reflux

conditions. The reaction was monitored by TLC. The formed precipitate was isolated by filtration. The product was dissolved in DMF (8 mL) and the catalyst was filtered. Then, water (5 mL) was added to the filtrate which resulted in the crystallization of the product. The resulting crystalline structure was filtered and dried with a vacuum pump. Spectral data of 4a and 4b compounds are presented:

Spectra data

5-((2-amino-5-methylphenyl)(2-nitrophenyl) methyl)-1,3-dimethylpyrimidine-2,4,6(1H,3H,5H)-trione (4a): Yellow solid. m. p. 183-185 °C. FT-IR (KBr): ν = 3324, 3319, 2920, 1688, 1552, 1352 cm^{-1}. – ^{1}H NMR (400 MHz, [D_6]DMSO): δ (ppm) = 2.98 (s, 3H, CH_3), 3.34 (s, 6H, $2CH_3$), 5.34 (d, J = 8.2 Hz, 1H, CH), 5.45 (d, J = 8.2 Hz, 1H, CH), 6.98-7.46 (m, 7H, ArH), 9.17 (s, 2H, NH_2). – ^{13}C NMR (100 MHz, [D_6]DMSO): δ (ppm) = 25.14, 31.74, 32.18, 43.72, 54.15, 121.22, 121.23, 125.18, 129.05, 129.12, 136.82, 136.84, 139.07, 142.21, 148.17, 154.16, 170.02.– Analysis for $C_{20}H_{20}N_4O_5$: calcd. C, 60.60, H, 5.09, N, 14.13; Found C, 60.54; H, 5.02; N, 14.03%.

5-((2-amino-5-methoxyphenyl)(4-(methylthio)phenyl)methyl)-1,3-dimethylpyrimidine-2,4,6(1H,3H,5H)-trione (4b): Yellow solid. m. p. 190-192 °C – IR (KBr): ν = 3412, 2915, 1682, 1491, 1443, 815 cm^{-1}. – ^{1}H NMR (400 MHz, [D_6]DMSO): δ (ppm) = 2.05 (s, 3H, CH_3), 2.48 (s, 3H, CH_3), 2.82 (s, 6H, $2CH_3$), 4.94 (d, J = 9.2 Hz, 1H, CH), 5.12 (d, J = 9.2 Hz, 1H, CH), 6.32-7.25 (m, 9H, ArH and NH_2). – ^{13}C NMR (100 MHz, [D_6]DMSO): δ (ppm) = 22.14, 27.92, 28.55, 50.52, 59.14, 64.55, 121.97, 124.93, 125.86, 126.07, 127.55, 127.93, 128.07, 135.04, 138.13, 139.84, 142.55, 148.73, 164.60, 169.62.– Analysis for $C_{21}H_{23}N_3O_4S$: calcd. C, 61.00, H, 5.61, N, 10.16, S, 7.75; Found C, 61.07, H, 5.74, N, 10.18, S, 7.84 %.

RESULTS AND DISCUSSION

A facile hydrothermal way was utilized for the preparation of N-GQDs [24]. Amino-functionalized graphene quantum dots were prepared using 3-aminopropyltriethoxysilane. XRD pattern of CuO/ZnO@N-GQDs@NH_2 nanocomposite is indicated in Fig. 1. XRD pattern confirms presence of both CuO (JCPDS No.80-1268) and ZnO (JCPDS No 80-0075).

SEM images of CuO/ZnO and CuO/ZnO@N-GQDs@NH_2 nanocomposite are indicated in Fig. 2. SEM images of the CuO/ZnO@N-GQDs@NH_2 nanocomposite presented the formation of uniform particles, and the energy-dispersive X-ray spectrum (EDS) confirmed the presence of Cu, Zn, N, O and C species in the structure of the nanocomposite (Fig. 3).

FT-IR spectra of CuO/ZnO, CuO/ZnO@N-

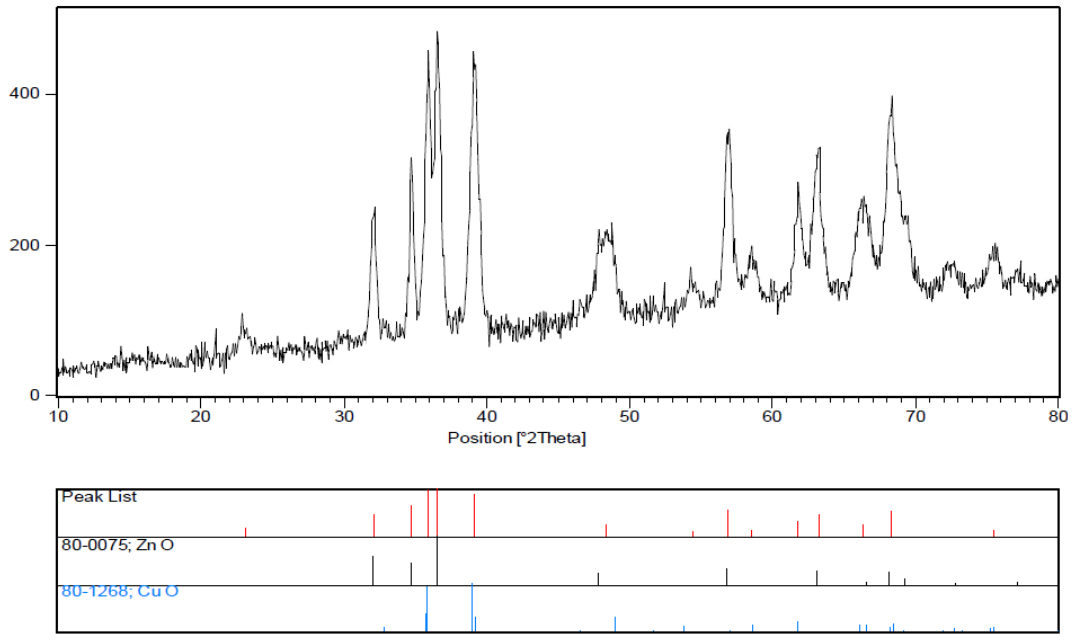

Fig 1. XRD pattern of CuO/ZnO@N-GQDs@NH_2

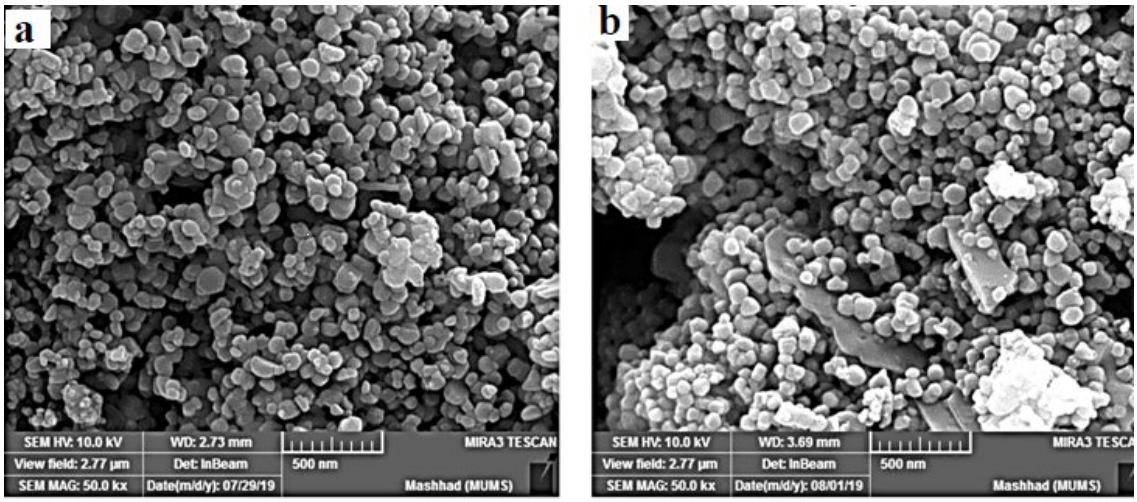

Fig 2. SEM images of (a) CuO/ZnO and (b) CuO/ZnO@N-GQDs@NH_2

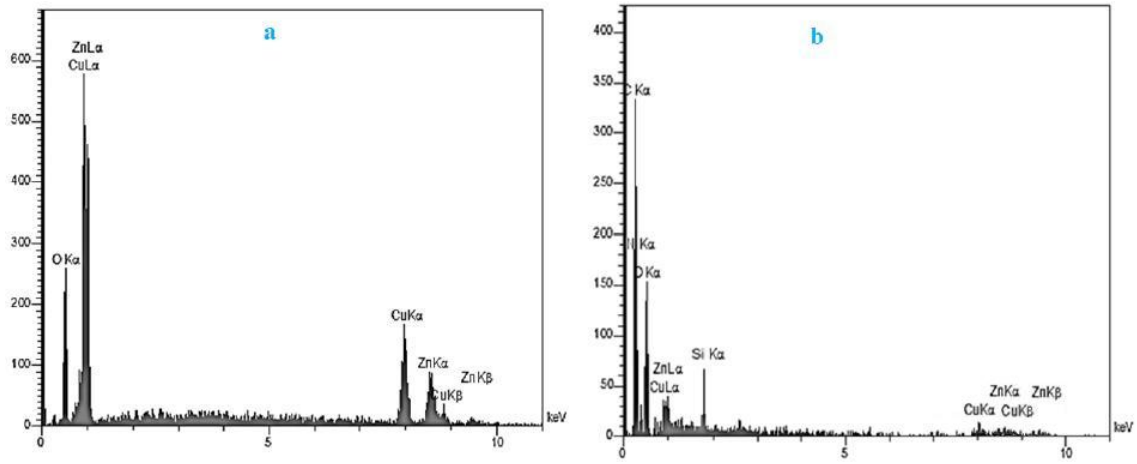

Fig 3. EDS spectra of (a) CuO/ZnO, and (b) CuO/ZnO@N-GQDs@NH_2

GQDs and CuO/ZnO@N-GQDs@NH_2 nanocomposite are shown in Fig. 4. The absorption peak at 3320 cm^{-1} is related to the stretching vibrational absorptions of OH. The peaks at 450 and 509 cm^{-1} corresponded to the Zn-O and Cu-O bonds, respectively. The characteristic peaks at 3400 cm^{-1} (O-H stretching vibration), 1660 cm^{-1} (C=O stretching vibration), 1100 cm^{-1} (C-O-C stretching vibration) appear in the spectrum of Figure 4b. The peak at approximately 1475-1580 cm^{-1} is attributed to C=C bonds. The peaks at 1560 and 3350cm^{-1} are related to the bending and stretching vibrational absorptions of N-H, respectively (Fig 4c).

Thermogravimetric analysis (TGA) considers the thermal stability of the CuO/ZnO@N-GQDs@NH_2 nanocomposites (Figure 5). The curve indicates a weight loss from 200 to 600 °C, that is attributed to the oxidation, degradation of N-GQD and decomposition of the organic spacer grafting to the N-GQD surface.

X-ray photoelectron spectroscopy (XPS) analysis of CuO/ZnO @N-GQDs@NH_2 nanocomposite was indicated in Figure 6. In the wide-scan spectrum of nanocatalyst, the predominant components are Zn2p (1030-1055 eV), Cu2p (940-970 eV), O 1s (530.8 eV), N 1s (400 eV) and C 1s (286.2 eV).

Generally, the peak centered at 284.5 eV is assigned to graphitic sp^2 C (C-C/C=C), the peaks located at 285.8 and 287.6 eV represent sp^3 C (C-C, C-O, C-N), and carbonyl C (C=O), and the peak

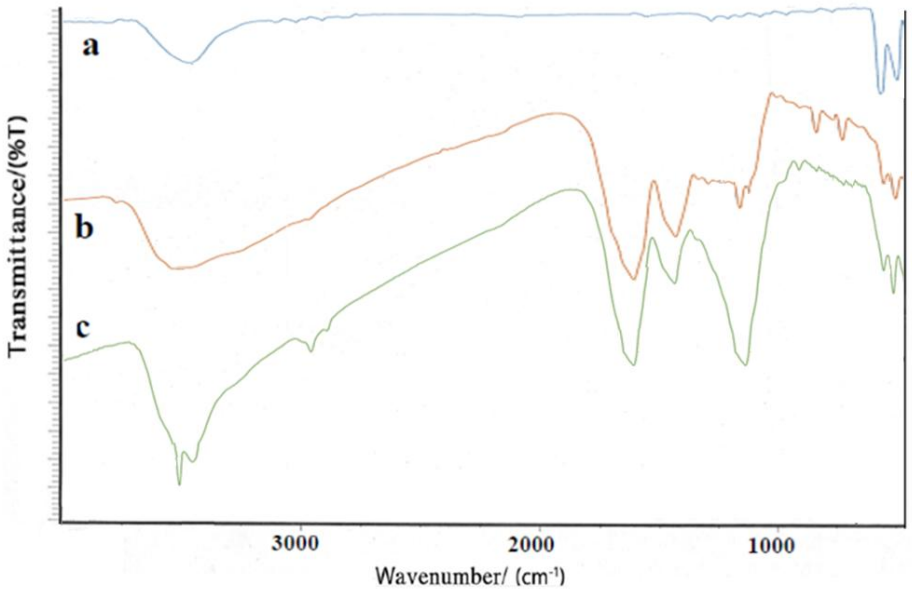

Fig 4. FT-IR of (a) CuO/ZnO, (b) CuO/ZnO@N-GQDs, and (c) CuO/ZnO@N-GQDs@NH_2

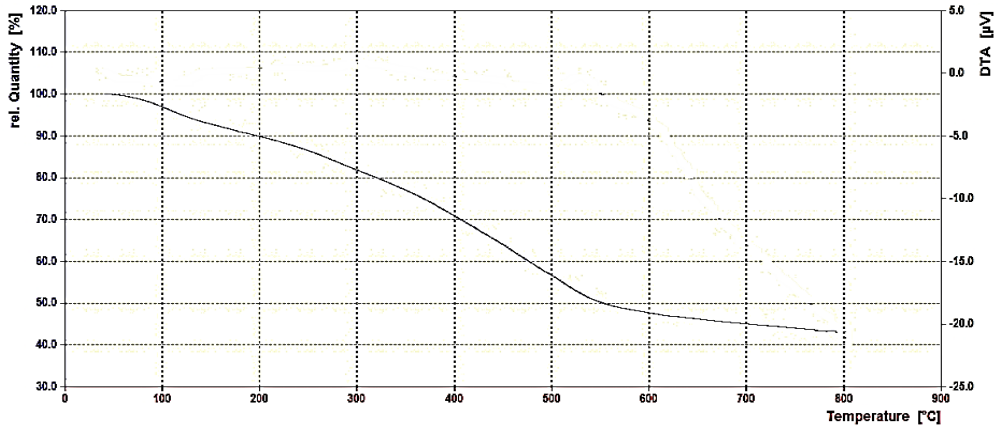

Fig 5. TGA of CuO/ZnO@N-GQDs@NH_2

at 288.5 eV is attributed to the carboxylate C(O)-O [25].

We commenced our investigation by testing the reaction of N,N-dimethylbarbituric acid, 4-chlorobenzaldehyde and 4-methoxy aniline as a model reaction. To obtain the ideal reaction conditions for the synthesis of compound **4c**, we studied the different catalysts and solvents which are shown in Table 1. Screening of diverse catalysts containing NiO, $NaHSO_4$, ZrO_2, Et_3N, CuO/ZnO, CuO/ZnO@N-GQDs and CuO/ZnO@N-GQDs@NH_2 nanocomposite revealed CuO/ZnO@N-GQDs@NH_2 nanocomposite (5 mg) as the most effective catalyst to perform this reaction under reflux condition in water (Table 1). Seeking of the reaction scope demonstrated that various aromatic aldehydes can be utilized in this method (Table 2). These results showed that aromatic aldehydes with electron-withdrawing groups reacted faster than aldehydes with electron-releasing groups as expected.

The reusability of CuO/ZnO@N-GQDs@NH_2 nanocomposite was tested for the synthesis of 4c and it was found that product yields reduced to a small extent on each reuse (run 1, 94%; run 2, 94%; run 3, 93%; run 4, 93%; run 5, 92%; run 6, 92%;).

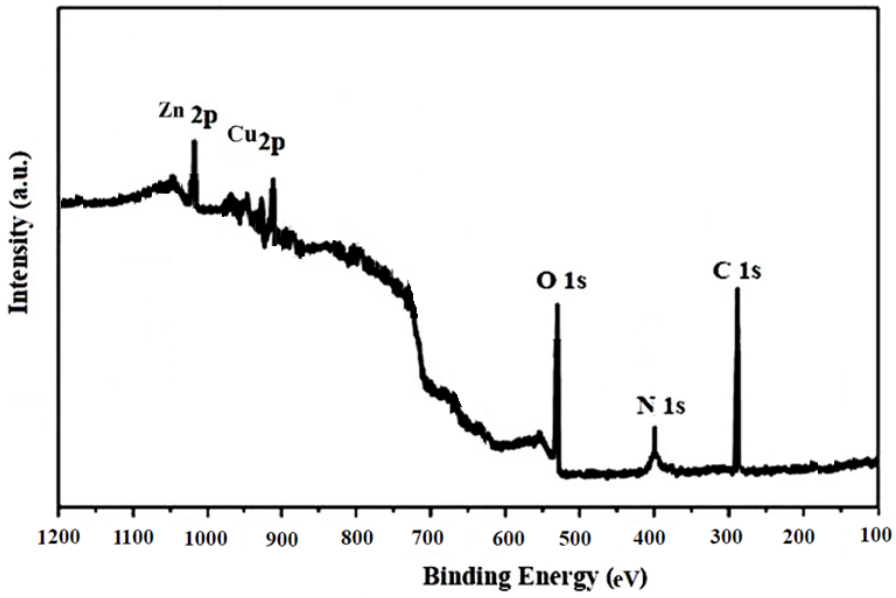

Fig 6. X-ray photoelectron spectroscopy (XPS) analysis of CuO/ZnO@N-GQDs@NH_2 nanocomposite

Table 1. Optimization of reaction conditions using different catalysts under different conditions [a]

Entry	Catalyst (amount)	Solvent (reflux)	Time (min)	Yield [b]%
1	--------	H_2O	400	trace
2	Et_3N (5 mol%)	H_2O	300	32
3	$NaHSO_4$ (4 mol%)	H_2O	180	45
4	NiO (8 mg)	H_2O	140	40
5	ZrO_2 (6 mg)	H_2O	140	50
6	CuO/ZnO (8 mg)	H_2O	100	52
7	CuO/ZnO@N-GQDs (5 mg)	H_2O	100	57
8	CuO/ZnO@N-GQDs@NH_2 nanocomposite (5 mg)	DMF	50	60
9	CuO/ZnO@N-GQDs@NH_2 nanocomposite (5 mg)	CH_3CN	50	74
10	CuO/ZnO@N-GQDs@NH_2 nanocomposite (5 mg)	EtOH	50	80
11	CuO/ZnO@N-GQDs@NH_2 nanocomposite (3 mg)	H_2O	50	85
12	CuO/ZnO@N-GQDs@NH_2 nanocomposite (5 mg)	H_2O	50	94
13	CuO/ZnO@N-GQDs@NH_2 nanocomposite (7 mg)	H_2O	50	94

[a] N,N-dimethylbarbituric acid (1 mmol), 4-chlorobenzaldehyde (1 mmol) and 4-methoxy aniline (1 mmol)
[b] Isolated yield

Table 2. Synthesis of pyrimidine-triones by CuO/ZnO@N-GQDs@NH_2 nanocomposite (5 mg)

Entry	R: (Aldehyde)	R′:(Aniline)	Product	Time (min)	Yield[a]%	M.p. (°C)
1	2-NO_2	4-CH_3	**4a**	50	89	183-185
2	4-SCH_3	4-OCH_3	**4b**	60	85	190-192
3	4-Cl	4-OCH_3	**4c**	50	94	240-242
4	3-NO_2	4-CH_3	**4d**	50	89	188-190
5	4-NO_2	4-OCH_3	**4e**	50	94	237-239
6	2,4-di-Cl	4-CH_3	**4f**	50	94	198-200
7	4-F	4-OCH_3	**4g**	50	90	222-224
8	4-CH_3	4-CH_3	**4h**	60	85	205-207

[a] Isolated yield

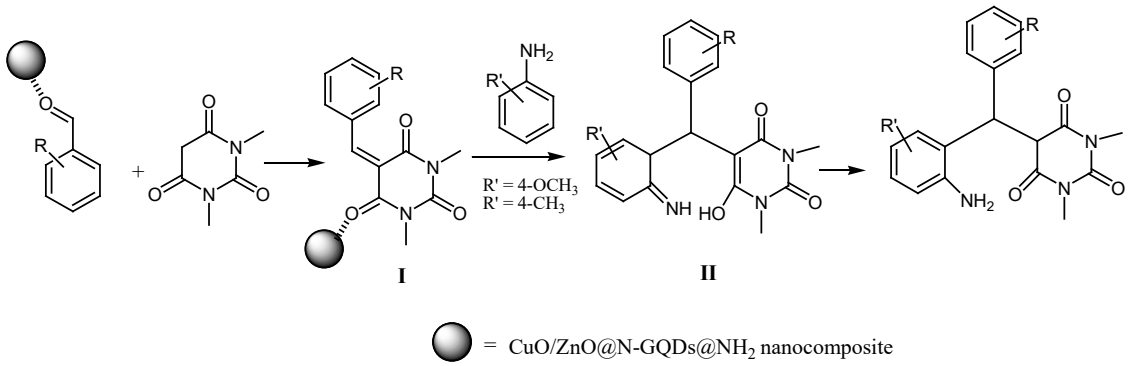

Scheme 2. Possible mechanism for the synthesis of pyrimidine-triones using CuO/ZnO@N-GQDs@NH_2 nanocomposite

A proposed mechanism for the synthesis of pyrimidine-triones using CuO/ZnO@N-GQDs@NH_2 nanocomposite is indicated in Scheme 2. At the start, N,N-dimethylbarbituric acid is reacted with benzaldehyde to form intermediate (I) *via* condensation reaction. Intermediate (I), in the presence of CuO/ZnO@N-GQDs@NH_2 nanocomposite, is condensed with aniline to form intermediate (II). The migration of the hydrogen atom will create the final product (Scheme 2).

CONCLUSION

In conclusion, we demonstrated an efficient way for the preparation of pyrimidine-triones through three-component reaction of N,N-dimethylbarbituric acid, benzaldehydes and para-methyl aniline or para-methoxy aniline under reflux condition in water. The salient features of this protocol are: great yields, concise reaction times, retrievability of the catalyst, and little nanocatalyst loading.

CONFLICT OF INTEREST

The authors confirm that this article content has no conflict of interest.

REFERENCES

1. El-Deeb IM, Lee SH. Design and synthesis of new anticancer pyrimidines with multiple-kinase inhibitory effect. Bioorganic & Medicinal Chemistry. 2010;18(11):3860-74.
2. Barakat A, Soliman SM, Al-Majid AM, Lotfy G, Ghabbour HA, Fun H-K, et al. Synthesis and structure investigation of novel pyrimidine-2,4,6-trione derivatives of highly potential biological activity as anti-diabetic agent. Journal of Molecular Structure. 2015;1098:365-76.
3. Kostova I, Atanasov PY. Antioxidant Properties of Pyrimidine and Uracil Derivatives. Current Organic Chemistry. 2017;21(20).
4. Mohamed MS, Kamel R, Fatahala SS. Synthesis and biological evaluation of some thio containing pyrrolo [2,3-d]Pyrimidine derivatives for their anti-inflammatory and anti-microbial activities. European Journal of Medicinal Chemistry. 2010;45(7):2994-3004.
5. Andrews PR, Jones GP, Lodge D. Convulsant, anticonvulsant and anaesthetic barbiturates. 5-Ethyl-5-(3′-methyl-but-2′-enyl)-barbituric acid and related compounds. European Journal of Pharmacology. 1979;55(2):115-20.
6. Sharma M, Borah P, Bhuyan PJ. ChemInform Abstract: InCl3-Catalyzed, Three-Component Reactions for the Synthesis of Some Novel Functionalized/Annulated Barbituric Acids. ChemInform. 2015;46(43):no-no.
7. Panahi F, Yousefi R, Mehraban MH, Khalafi-Nezhad A. Synthesis of new pyrimidine-fused derivatives as potent and selective antidiabetic α-glucosidase inhibitors. Carbohydrate Research. 2013;380:81-91.
8. Azzam SHS, Pasha MA. Microwave-assisted, mild, facile, and rapid one-pot three-component synthesis of some novel pyrano[2,3-d]pyrimidine-2,4,7-triones. Tetrahedron Letters. 2012;53(52):7056-9.
9. Rahmati A, Khalesi Z. A one-pot, three-component synthesis of spiro[indoline-isoxazolo[4′,3′:5,6]pyrido[2,3-d]pyrimidine]triones in water. Tetrahedron. 2012;68(40):8472-9.
10. Shirvan SA, Ghahremanzadeh R, Moghaddam MM, Bazgir A, Zarnani AH, Akhondi MM. A Novel Method for the Synthesis of Spiro[indoline-Pyrazolo[4′,3′:5,6]pyrido[2,3-d] pyrimidine]triones by Alum as a Reusable Catalyst. Journal of Heterocyclic Chemistry. 2012;49(4):951-4.
11. Safaei-Ghomi J, Shahbazi-Alavi H. Synthesis of dihydrofurans using nano-CuFe2O4@Chitosan. Journal of Saudi Chemical Society. 2017;21(6):698-707.
12. Misra M, Kapur P, Nayak MK, Singla M. Synthesis and visible photocatalytic activities of a Au@Ag@ZnO triple layer core–shell nanostructure. New J Chem. 2014;38(9):4197-203.
13.Roushani M, Valipour A, Bahrami M. The potentiality of the functionalized nitrogen and thiol-doped graphene quantum dots (GQDs-N-S) to stabilize the antibodies in the designing of human chorionic gonadotropin immunosensor. Nanochemistry Research. 2019;4(1):20-6.
14.Singh R, Kumar M, Tashi L, Khajuria H, Sheikh HN. Hydrothermal synthesis of nitrogen doped graphene supported cobalt ferrite (NG@CoFe2O4) as photocatalyst for the methylene blue dye degradation. Nanochemistry Research. 2018;3(2):149-59.
15. Yan Y, Gong J, Chen J, Zeng Z, Huang W, Pu K, et al. Recent Advances on Graphene Quantum Dots: From Chemistry and Physics to Applications. Advanced Materials. 2019;31(21):1808283.

16. Du Y, Guo S. Chemically doped fluorescent carbon and graphene quantum dots for bioimaging, sensor, catalytic and photoelectronic applications. Nanoscale. 2016;8(5):2532-43.
17. Hu E, Yu X-Y, Chen F, Wu Y, Hu Y, Lou XWD. Graphene Layers-Wrapped Fe/Fe5 C2 Nanoparticles Supported on N-doped Graphene Nanosheets for Highly Efficient Oxygen Reduction. Advanced Energy Materials. 2017;8(9):1702476.
18. Hu E, Feng Y, Nai J, Zhao D, Hu Y, Lou XW. Construction of hierarchical Ni–Co–P hollow nanobricks with oriented nanosheets for efficient overall water splitting. Energy & Environmental Science. 2018;11(4):872-80.
19. Li M, Chen T, Gooding JJ, Liu J. Review of Carbon and Graphene Quantum Dots for Sensing. ACS Sensors. 2019;4(7):1732-48.
20. Wang Z, Zeng H, Sun L. Graphene quantum dots: versatile photoluminescence for energy, biomedical, and environmental applications. Journal of Materials Chemistry C. 2015;3(6):1157-65.
21. Shahbazi-Alavi H, Safaei-Ghomi J. Synthesis of pyrimidines using nano-NiZr4 (PO4)6 as a retrievable and robust heterogeneous catalyst. Nanochemistry Research. 2020;5(2):141-7.
22. Bodaghifard MA, Faraki Z, Asadbegi S. Effective fabrication of poly(anilin-formaldehyde)-supported hybrid nanomaterial and catalytic synthesis of dihydropyridines. Nanochemistry Research. 2019;4(2):101-11.
23. Taghavi Fardood S, Moradnia F, Ghalaichi AH, Danesh Pajouh S, Heidari M. Facile green synthesis and characterization of zinc oxide nanoparticles using tragacanth gel: investigation of their photocatalytic performance for dye degradation under visible light irradiation. Nanochemistry Research. 2020;5(1):69-76.
24. Qu D, Zheng M, Du P, Zhou Y, Zhang L, Li D, et al. Highly luminescent S, N co-doped graphene quantum dots with broad visible absorption bands for visible light photocatalysts. Nanoscale. 2013;5(24):12272.
25. Qu D, Zheng M, Li J, Xie Z, Sun Z. Tailoring color emissions from N-doped graphene quantum dots for bioimaging applications. Light: Science & Applications. 2015;4(12):e364-e.